Mechanosensitive currents in the neurites of cultured mouse sensory neurones

Jing Hu and Gary R. Lewin

Department of Neuroscience, Max-Delbrück Center for Molecular Medicine and Charité Universitätsmedizin Berlin, Robert-Rössle-Str. 10, Berlin-Buch D-13125, Germany

Almost all sensory neurones in the dorsal root ganglia have a mechanosensory function. The transduction of mechanical stimuli *in vivo* takes place exclusively at the sensory ending. For cutaneous sensory receptors it has so far proved impossible to directly record the mechanically gated receptor potential because of the small size and inaccessibility of the sensory ending. Here we investigate whether mechanosensitive currents are present in the neurites of freshly isolated adult mouse sensory neurones in culture. Amost all sensory neurone neurites possess currents gated by submicrometre displacement stimuli (92%). Three types of mechanically activated conductance were characterized based on different inactivation kinetics. A rapidly adapting conductance was found in larger sensory neurones with narrow action potentials characteristic of mechanoreceptors. Slowly and intermediate adapting conductances were found exclusively in putative nociceptive neurones. Mechanically activated currents with similar kinetics were found also after stimulating the cell soma. However, soma currents were only observed in around 60% of cells tested and the displacement threshold was several times larger than for the neurite ($\sim$6 μm). The reversal potential of the rapidly adapting current indicated that this current is largely selective for sodium ions whereas the slowly adapting current is non-selective. It is likely that distinct ion channel entities underlie these two currents. In summary, our data suggest that the high sensitivity and robustness of mechanically gated currents in the sensory neurite make this a useful *in vitro* model for the mechanosensitive sensory endings *in vivo*.

(Received 20 July 2006; accepted after revision 6 October 2006; first published online 12 October 2006)
Corresponding author G. R. Lewin: Max-Delbrück Center for Molecular Medicine and Charité Universitätsmedizin Berlin, Robert-Rössle-Str. 10, Berlin-Buch D-13125, Germany. Email: glewin@mdc-berlin.de

Our senses of touch, pain and proprioception all rely on the ability of primary sensory neurones to rapidly transform mechanical forces into electrical signals. This fundamental sensory transduction step still remains a puzzle at the cellular and molecular level (Gillespie & Walker, 2001; Lewin & Moshourab, 2004). It is thought that mechanical forces on sensory nerve endings directly open ion channels in the membrane and thus depolarize and excite the neurone (Loewenstein & Skalak, 1966; Lewin & Moshourab, 2004). In mammals, the only mechanoreceptors from which a mechanically gated receptor potential has been measured *in vivo* are Pacinian corpuscles and muscle spindle afferents (Loewenstein & Skalak, 1966; Hunt & Ottoson, 1973). For most other sensory afferents, the very small size and extreme inaccessibility of the mechanosensitive peripheral endings have precluded direct extracellular or intracellular recordings of electrical events evoked by mechanical stimulation of the ending (Hu *et al.* 2006).

An alternative approach is to ask whether adult sensory neurones cultured for short periods might possess mechanosensitive channels, as these cells are accessible for high-resolution recordings of membrane currents using the whole-cell patch-clamp technique. Experiments have been carried out on cultured dorsal root ganglion (DRG) neurones with negative pressure applied through the recording pipette to activate channels that are presumably gated by the resulting stretch of the patched membrane (Cho *et al.* 2002). Using this methodology, three distinct types of cation-permeable channels with different pressure thresholds have been characterized. They have been termed high threshold, low threshold and low threshold small conductance channels (Cho *et al.* 2002, 2006). However, the activation kinetics of these channels

 DOI: 10.1113/jphysiol.2006.117648

was found to be slow, of the order of seconds, and this time course is inconsistent with the finding that mechanoreceptors respond with very short latencies (2–10 ms) to mechanical stimulation (Shin *et al.* 2003). Others have used direct mechanical stimulation of the cell soma to open mechanically activated channels whose activation can be measured under voltage-clamp conditions (Cunningham *et al.* 1995; McCarter *et al.* 1999; Drew *et al.* 2002, 2004; Di Castro *et al.* 2006). Using this approach, both rapidly inactivating and slowly inactivating mechanically gated conductances have been characterized in cultured neonatal and adult sensory neurones (McCarter *et al.* 1999; Drew *et al.* 2002, 2004). One potential drawback is that in the intact *in vivo* situation it is only the peripheral endings of sensory neurones not the cell body that displays mechanosensitivity. Here we hypothesize that mechanosensitive ion channels are present in the neurites of cultured neurones and that their physiological properties might better match the *in vivo* situation. We show that the vast majority of adult sensory neurones possess exquisitely sensitive mechanically gated conductances on their neurites *in vitro*. These conductances are gated very rapidly and are probably underpinned by at least two distinct types of mechanosensitive channel that are preferentially expressed by low and high threshold mechanoreceptors.

Methods

Cell culture

DRG neurones from adult mouse were prepared essentially as previously described (Mannsfeldt *et al.* 1999; Stucky *et al.* 2002). No nerve growth factor or other neurotrophin was added to the medium. DRG from all spinal levels were removed from adult C57/Bl6 mice, and neurones were isolated and cultured based on previously published protocols (Lindsay, 1988). Mice were killed by placement in a CO_2-filled chamber for a 2–4 min followed by cervical dislocation. Animal housing and care, as well as protocols for killing, are registered with and approved by the appropriate German federal authorities (State of Berlin). The DRG neurones were incubated with 1 mg ml^{-1} collagenase IV (Sigma, St Louis, MO, USA) and 0.05% trypsin (Sigma) for 30 min each at 37°C. The DRG neurones were suspended in DMEM/Hams-F12 medium (Life Technologies, Gaithersburg, MD, USA) containing 10% heat-inactivated horse serum (Biochrom), 20 mM glutamine, 0.8% glucose, 100 U penicillin and 100 mg ml^{-1} streptomycin (Life Technologies). DRG neurones were mechanically dissociated into a suspension of single cells by passing them through fire-polished Pasteur pipettes. The cells were then spot-plated on poly-L-lysine (200 mg ml^{-1})–laminin (20 μg ml^{-1})-coated coverslips (1000–2000 cells per coverslip), and maintained at 37°C in 5% CO_2. The median time in culture was 24 h (range, 16–48 h).

Whole-cell patch-clamp recordings from isolated DRG neurones

Whole-cell recordings were made from DRG neurones using fire-polished glass electrodes with a resistance of 3–5 MΩ. Extracellular solution contained (mM): NaCl 140, $MgCl_2$ 1, $CaCl_2$ 2, KCl 4, glucose 4 and Hepes 10 (pH 7.4), and electrodes were filled with solution containing (mM): KCl 110, Na^+ 10, $MgCl_2$ 1, EGTA 1 and Hepes 10 (pH 7.3). For most experiments, 0.1% Lucifer Yellow was included in the electrode. Cells were perfused with drug-containing solutions by moving an array of outlets in front of the patched cells (Biologic). TTX was prepared in a final concentration of 1 or 10 μM in extracellular solution.

Observations were made with Axiovert200 equipped with TILL imaging system, including the polychome V, a CCD camera and the imaging software TILLvisION. The measurement of soma size was carried out *post hoc* using digital photographs of each recorded cell. The diameter of each soma was calculated from the mean of the longest and shortest diameters. Membrane current and voltage were amplified and acquired using an EPC-9 amplifier sampled at 10–40 kHz; signals were analysed using Pulse and PulseFit software (HEKA). Pipette and membrane capacitance were compensated using the auto function of Pulse. To minimize the voltage error, 70% of the series resistance was compensated. For most experiments the membrane voltage was held at −60 mV with the voltage-clamp circuit. After establishing whole-cell configuration, voltage-gated currents were measured using a standard series of voltage commands. Briefly, the neurones were prepulsed to −120 mV for 150 ms and depolarized from −50 to +50 mV in increments of 5 mV (40 ms test pulse duration). Next the amplifier was switched to current-clamp mode and action current injection was used to evoke action potentials (pulses varied from 0.02 to 10 nA for 80 ms). The same procedure was repeated during continuous superfusion of the single cell with 1 μM TTX. After confirmation that the action potential was blocked in the presence of TTX, the recording mode was switched back to voltage clamp to record mechanically activated inward currents at a holding potential of −60 mV. In between the mechanical stimuli TTX was removed to check that the cell was still healthy by recording action potential and voltage-gated currents in current- and voltage-clamp modes. If the membrane capacitance and resistance changed more than 20% after the mechanical stimulus, the cell was regarded as membrane damaged and the data discarded.

Mechanical stimuli were applied using a heat-polished glass pipette (tip diameter, 2–5 μm), driven by MM3A Micromanipulator system (Kleindiek Nanotechnik,

Reutlingen), positioned at an angle of 45 deg to the surface of the dish. The nanomotor is a very small piezo-based motor that has two modes of operation: the coarse and the fine mode. In the coarse mode the motor moves a slider very rapidly in single steps. The size of a single coarse step has to be measured for each individual manipulator and system configuration. Calibration of the single-step size can be done relatively simply by instructing the motor to move a large number of steps (500, 1000, 2000, etc.) and measuring the total distance moved. The velocity of the motor can be set by changing frequency, which controls how rapidly the piezo crystal is activated. The maximum stable velocity of movement for 1 μm was 10 μm ms^{-1}. Because of changes in the system configuration, the velocity of the 0.75 μm step was 2.8 μm ms^{-1}. The voltage signal sent to the nanomotor by the control unit was simultaneously fed into a second channel of the EPC9 amplifier so that the timing of the nanomotor movement in relation to the mechanically activated current could be accurately determined. The nanomotor has a second so-called fine mode in which the maximum movement is 1000 fine steps which corresponds approximately to 1000 nm. The speed of movement in the fine mode was set to 10 μm ms^{-1}. The nanomotor device was tested for the accuracy and speed of the displacement stimuli by measuring actual movement of the tip with a laser interferometre.

For the experiment, the probe was positioned near the neurite or cell body, moved forward in steps of 0.75 or 1.0 μm (with the velocities indicated above) for 230 ms and then withdrawn; stimulus amplitude can be directly controlled using macro-based software commands. If there was no response, the probe was moved forward again and the same procedure was repeated until a mechanically activated inward current was recorded. We have analysed the data using a 0.75 and 1.0 μm step together because both the mean amplitude of the mechanically gated currents and the measured kinetic parametres of the currents were not statistically different. It should be noted, however, that the majority of the data was obtained using the 0.75 μm step (99/158 cells recorded). For the analysis of the kinetic properties of mechanically activated current, traces were fitted with single-exponential functions using Pulsefit (HEKA). Data are presented as means ± S.E.M. All electrophysiological experiments were carried out between 12 and 48 h after plating.

To test the voltage dependence of the mechanosensitive currents, the cell soma was mechanically stimulated under voltage-clamp conditions. It was important in these experiments to ensure that the mechanically activated current was of constant amplitude with repeated stimulation. The membrane voltage was then set manually to various membrane voltages for several tens of seconds before the application of the mechanical stimulus. At all holding potentials special care was taken to ensure that any voltage-activated outward or inward currents had inactivated before application of the stimulus.

Results

Mechanosensitive conductances in sensory neurone neurites

We tested whether mechanical stimulation of sensory neurites of neurones grown on a poly-L-lysine–laminin substrate could evoke fast inward currents (Fig. 1). In the first series of experiments, we used the coarse mode of the manipulator to stimulate cultivated sensory neurones. In almost all cases (146/158) a small mechanical stimulus (0.75 or 1.0 μm displacement, see Methods) of the neurite evoked a fast inward current measured at the voltage-clamped (−60 mV) cell soma (Fig. 1). In most cases the neurone was loaded with Lucifer yellow delivered through the patch pipette so that neurites belonging to the recorded neurone could be unequivocally identified (Fig. 1*A*). Recordings were made between 12 and 48 h after plating and we noted no systematic change in the incidence of mechanosensitive currents within this time period. It should be noted that the single step used in each case represents the maximum possible membrane displacement because the probe starting position in relation to the neurite membrane cannot be determined. Thus the actual membrane displacement for each effective stimulus is a value somewhere between 0 and 1000 nm. The actual minimum membrane displacement needed to evoke a mechanically gated current is likely to be in the range of 200 nm (see below). Consistent with this, the effective single-step mechanical stimulus did not lead to visible movement of the stimulated neurite.

We found that in many cases the small mechanical stimuli used to stimulate neurites were capable of initiating action potentials (Fig. 2). Indeed in some cases when we mechanically stimulated the cell soma (see below) we also evoked action potentials (data not shown). Therefore currents were routinely measured in the presence of TTX to minimize the contribution from voltage-gated channels. The single-step mechanical displacement of the neurite (0.75 or 1.0 μm) evoked a mechanically gated current with kinetics that allowed its classification into one of three types. Many cells with larger cell diameters displayed a rapidly adapting (RA) current that activates and inactivates very quickly (Figs 1*B* and *C* and 2, and Table 1). These currents were of large amplitude (mean peak amplitude, ∼400 pA); the size of the current was particularly surprising considering the small area of membrane stimulated. The second type of current we observed was intermediate adapting (IA), which also activates very rapidly but shows a much slower rate of inactivation. The mean peak amplitude of the IA current was again large and not significantly different from the mean amplitude of the RA current (Table 1).

The IA mechanically activated current was also relatively rare (16/158 recorded cells) (Fig. 3). The third type of mechanically activated current was slowly adapting (SA), this current inactivated only marginally during the 230 ms long stimulus given here (Fig. 1*B* and Table 1). Cells with an SA current response were on average smaller than RA cells and this difference was statistically significant ($P < 0.05$, unpaired t test) (Table 1 and Fig. 3).

We examined the kinetic properties of the mechanically activated current. We measured the latency between onset of probe movement and current activation (Fig. 1*C* and *D*). In cells displaying RA, SA or IA responses, the current activated very rapidly (400–800 μs) and there was no significant difference in latency between the RA and SA current types (Fig. 1*D*). However, for cells with an IA current, the measured latency for current activation was around half that measured for cells with an RA or SA currents and this difference was significant ($P < 0.01$, unpaired t test) (Fig. 1*D*). The latency estimates represent an upper bound on the actual latency as the latency between command voltage and probe movement is not known but may be significant. We therefore presume that the actual latency for channel gating may be significantly less than the fastest measured values of ~400 μs. We could fit the current traces with single exponential functions for activation and inactivation and calculate a time constant for current activation (τ_1) and inactivation (τ_2). It is interesting that τ_1 values were around 1 ms or less (Table 1). The mean τ_1 values for RA and SA current were not different but interestingly the activation time constant of the IA current was significantly faster at around 500 μs (Table 1). A time constant for inactivation could only be plotted for RA and IA currents as the SA current did not decay significantly during the 230 ms long stimulus given here. The time constant for inactivation of the RA current was very fast (1.68 ± 0.14 ms, $n = 65$); in contrast, the time constant for the IA current (25.87 ± 6.41 ms, $n = 16$), was 10-fold slower than the RA current. We also noticed that when an SA current was evoked a significant inward current was observed for tens of milliseconds after the withdrawal of the mechanical stimulus (Figs 1*A* and 2*A*). The submillisecond latency and activation kinetics of all three currents strongly indicates that the mechanical stimulus directly gates ion channels without any intervening enzymatic step. Furthermore, almost all (92%) DRG neurones in culture possess one of three kinetically distinct mechanically activated conductances on their neurites that can be activated by submicrometre displacement stimuli.

Action potentials are initiated by mechanical stimulation of the neurite

In many cases we recorded mechanosensory responses before and after the addition of TTX. We made recordings in current-clamp mode and observed the arrival of action

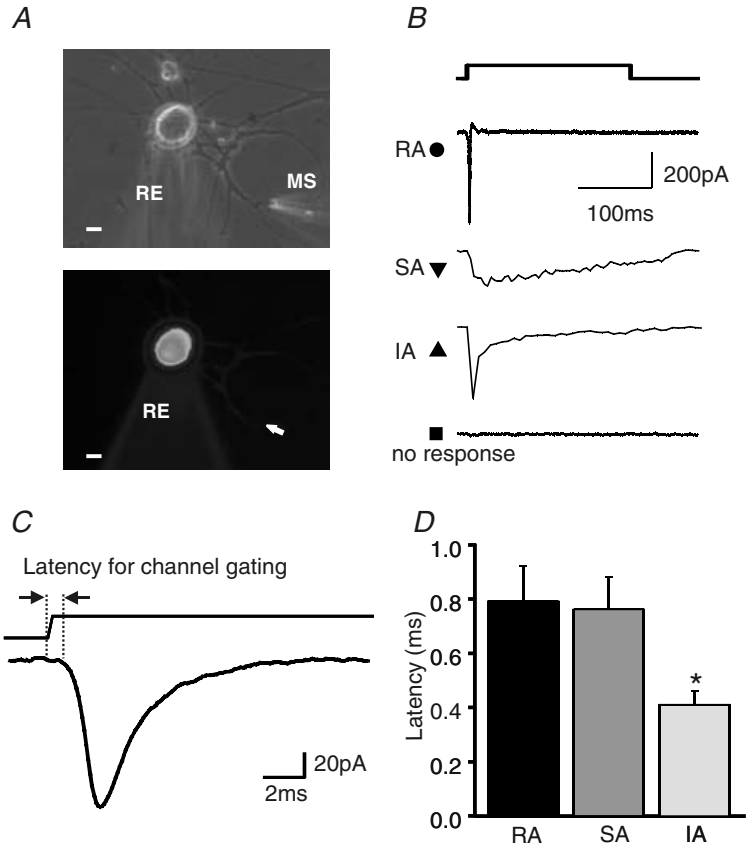

Figure 1. Mechanosensitivity of DRG neurones cultured on poly-L-lysine–laminin substrate
A, images of single DRG neurone in the whole-cell recording configuration with the mechanical stimulator (MS) poised to stimulate one of the neurites. Phase-contrast image (top) and fluorescent image (bottom). The cell and neurites were loaded with Lucifer Yellow dye via the recording electrode (RE). The arrow shows the site of stimulation with the MS. Scale, 10 μm. *B*, sample traces of the different types of mechanically gated currents obtained. RA, rapidly adapting; SA, slowly adapting; IA, intermediate adapting. *C*, example of an RA current drawn on an expanded scale showing how mechanical latency was measured. *D*, the mean mechanical latency for RA, IA and SA currents are shown. The mean measured latency for the RA and SA current was not different but IA currents were activated with significantly shorter latencies than both RA and SA currents (*$P < 0.01$, unpaired t test).

potentials in the soma following mechanical stimulation of the neurite (data not shown). The mean distance from the point of neurite stimulation to the soma was 76.1 ± 3.2 μm for all cells recorded. In most cases the soma was voltage clamped and we observed very large inward currents that probably reflect the arrival of action potentials in the voltage-clamped cell soma from the site of mechanical stimulation on the neurite (Fig. 2). We found that after application of TTX, one of the three types of currents (RA, SA or IA) was observed. It is interesting that the amount of measured receptor current apparently needed to evoke action potentials in the neurite could be surprisingly small. For example, in cells with IA or SA responses, mechanically activated currents with peak amplitudes of 30 pA or less were found after addition of TTX (Fig. 2). We found that in cells with RA currents the latency for action potential initiation was very short but in IA and SA cells there was often an appreciable delay of several milliseconds before action potential initiation compared to the very short latency mechanically gated current (Fig. 2). In the presence of 1 μM TTX, a minority of cells with an SA current fired an action potential to somal current injection (13/65 cells). Mechanical stimulation of the neurites, however, did not evoke an action potential in these cells consistent with the elevated voltage threshold for activation of voltage-gated sodium channels in the presence of TTX.

As currents were recorded at the voltage-clamped soma approximately 70 μm from the site of stimulation, the question arises whether the kinetics of the measured current are significantly affected by active conductances or passive filtering in the neurite between the site of stimulation and recording. We tested this possibility by comparing the kinetic properties of mechanically evoked currents produced by stimulating neurites immediately adjacent (< 5 μm) to the cell soma or 70 μm distant. No action potentials could be produced by mechanically stimulating the neurite adjacent to the cell soma making it likely that the membrane was within the range of the voltage clamp. The amplitude, activation and inactivation kinetics of the three types of current measured after mechanical stimulation of the neurite near to the soma were indistinguishable from those found when stimulating a more distant neurite (Table 1). Thus the mechanically activated current recorded at the soma is an accurate reflection of the current activated even at distant neurite stimulation sites (70 μm) under normal circumstances.

Expression of the mechanically activated current in mechanoreceptors and nociceptors

We next asked whether different mechanically activated currents are distributed preferentially in mechanoreceptors as opposed to sensory neurones with a nociceptive function. Most nociceptors are sensitive to mechanical stimuli as well as other modalities of noxious stimuli (Lewin & Moshourab, 2004). It was clear that RA currents were potentially present in low-threshold mechanoreceptors as these cells were on average larger than the other recorded cells (Table 1). We used two other criteria to tentatively classify these cells as mechanoreceptors or nociceptors. First, in most cases an action potential was evoked in current clamp, either using mechanical stimuli or current injection, we counted the number of cells with a well-defined hump on the falling phase of the spike and these were identified as probable nociceptors (Koerber *et al.* 1988; Lawson *et al.* 1997; Stucky & Lewin, 1999; Fang *et al.* 2005). In a subpopulation of cells, we also measured the presence of TTX-insensitive voltage-gated sodium currents, which is characteristic of nociceptors. Thus if all fast, voltage-gated sodium currents were blocked by 1 μM TTX, the cells were classified as probable non-nociceptors. Cells displaying significant voltage-gated sodium currents in the presence of 1 μM TTX are on the other hand very likely to be nociceptors as

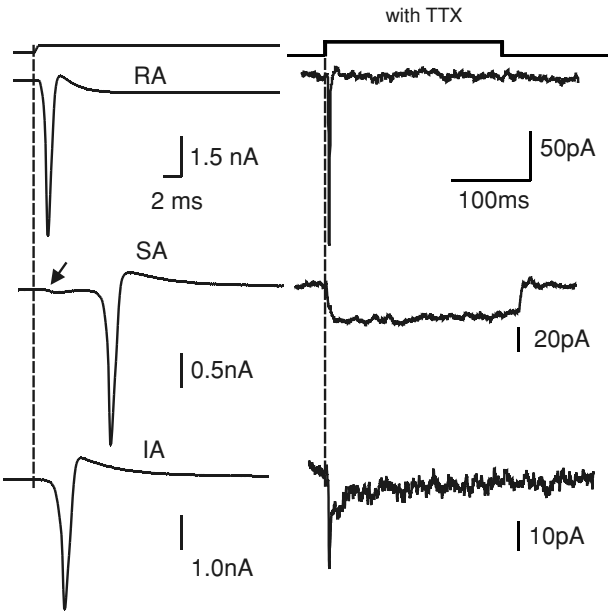

Figure 2. Mechanically activated currents before and after application of TTX
Sample current traces on the left show the whole-cell recording in the absence of TTX for three cells. The membrane potential at the cell soma was clamped at −60 mV. In each case a large transient inward current with a variable latency was evoked by the mechanical stimulus that probably represents the arrival of an unclamped action potential at the cell soma. Note that each cell could subsequently be classified as possessing an RA, SA or IA current after the response was evoked in the presence of TTX (right). Note that the amplitude and kinetics of the mechanically activated currents differ significantly from those observed in the absence of TTX (1 μM). Note that for the neurone that possessed an SA current (middle traces), the beginning of inward current activation can be seen to precede the action potential when recorded in the absence of TTX (arrow).

Table 1. Kinetic properties of the mechanosensitive current

	Neurite stimulation $n = 158$	Neurite stimulation (adjacent to cell body) $n = 12$	Cell body stimulation $n = 55$
RA cells	$n = 65$	$n = 6$	$n = 16$
Mean soma size (μm)	27.6 ± 0.8 (18–46 μm)	32.9 ± 3.4 (19–42 μm)	28.4 ± 1.2 (21–40 μm)
Mean current amplitude (pA)	385.2 ± 56.2	485.5 ± 226.5	327.4 ± 74.8
Activation τ_1 (ms)	1.04 ± 0.17	0.76 ± 0.21	0.86 ± 0.14
Inactivation τ_2 (ms)	1.68 ± 0.14	1.92 ± 0.39	1.05 ± 0.29‡
SA cells	$n = 65$	$n = 4$	$n = 14$
Mean soma size (μm)	24.0 ± 0.7* (15–41 μm)	32.4 ± 3.8 (23–41)	23.1 ± 1.4* (15–32 μm)
Mean current amplitude (pA)	234.0 ± 27.0	184.6 ± 101.6	377.1 ± 179.3
Activation τ_1 (ms)	1.28 ± 0.22†	0.96 ± 0.47	0.43 ± 0.07†
IA cells	$n = 16$	$n = 2$	$n = 4$
Mean soma size (μm)	28.2 ± 1.8 (16–44 μm)	32.0 ± 4.0 (28–36 μm)	24.0 ± 1.9 (19–28 μm)
Mean current amplitude (pA)	339.3 ± 77.4	529.0 ± 382.6	245.4 ± 67.4
Activation τ_1 (ms)	0.51 ± 0.11‡	0.67 ± 0.46	0.63 ± 0.19
Inactivation τ_2 (ms)	25.87 ± 6.41	17.18 ± 10.12	23.10 ± 9.4
No response	$n = 12$	$n = 0$	$n = 21$
Mean soma size (μm)	23.5 ± 1.4* (15–33 μm)	— —	24.9 ± 1.8* (16–44 μm)

*Soma size is significantly smaller than RA cells, $P < 0.01$ unpaired t test. †activation time constant τ_1 of the SA current in the soma is faster than that measured in the neurite, $P < 0.01$ unpaired t test. ‡activation time constant τ_1 for the IA current is significantly faster that found for the SA or RA current, $P < 0.01$ unpaired t test.

this indicates the presence of nociceptor-specific sodium channels (Akopian *et al.* 1996; Stucky & Lewin, 1999; Wood *et al.* 2004). Using this criterion, 59% of the cells with an RA current (17/29 cells) were classified as mechanoreceptors and the rest were classified as nociceptors. On the basis of such measurements, we subdivided cells with an RA current into two types: type 1 cells which have a non-nociceptive character, narrow action potentials and lack of TTX-insensitive sodium currents (Fig. 3*A*); and type 2 cells which mostly have a clear hump on the falling phase of the action potential and often possess significant TTX-resistant sodium channels (Fig. 3*A*). Cells with an SA mechanically activated current were also very common and these cells were usually of small size (Fig. 3 and Table 1). Consistent with this finding, all of these cells had nociceptor characteristics as assessed by action potential shape (91% (49/54) cells tested had an action potential with a hump) or the presence of TTX-insensitive sodium currents (73% (16/22) cells tested possessed TTX resistant sodium channels). Cells with IA currents were relatively rare but 70% (7/10) cells tested had an action potential with a hump (Fig. 3*A* and *B*) and 56% (5/9) cells tested had TTX-resistant sodium channels.

Overall it is clear that cells that are highly likely to be mechanoreceptors, based on a very narrow action potential and large soma size, possess large RA currents and we have called these cells RA type 1 cells (Fig. 3). It is interesting that about two-thirds of cells displaying an RA current were potentially nociceptors as they possess broad action potentials and have a significantly smaller soma size than type 1 cells (Fig. 3). The mean peak amplitude of the RA current in type 1 and type 2 cells as well as the latency for current activation was not different. However we did find that the RA current in type 1 cells activated and inactivated significantly faster than the current in type 2 cells (Fig. 3*C*). The remaining cells recorded with an IA or SA current were almost certainly nociceptors based on their broad humped action potentials and small soma size (Fig. 3). It was interesting to note, however, that the mean action potential width of cells with an IA current or type 2 cells with an RA current were practically identical. These cell types differed in that IA cells were clearly larger than both SA and type 2 RA cells (Fig. 3*B*).

In the case of nociceptors, it might be that the mechanosensitive SA current measured could be contaminated by a significant TTX-resistant sodium current often found in such cells (see above). However, in the presence of TTX we never observed currents that inactivate within tens of milliseconds as in classical TTX-resistant voltage-gated channels (Stucky & Lewin, 1999; Wood *et al.* 2004). We also saw no difference in the SA current even when we raised the TTX concentration to 10 μM. Furthermore, in every case tested the SA current reversed

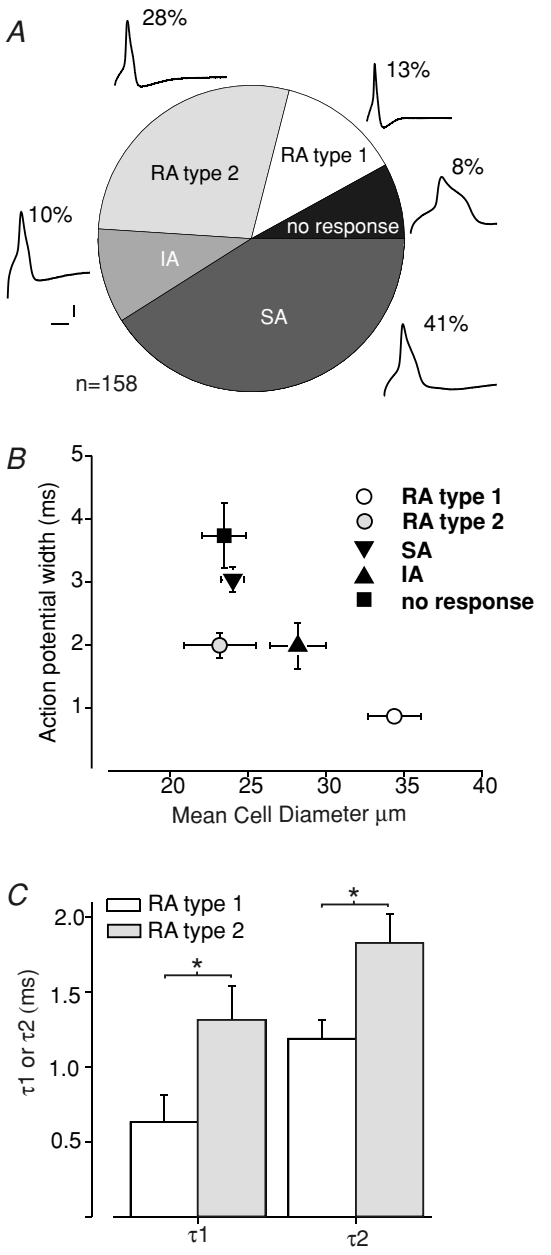

Figure 3. Expression of the mechanically activated current in mechanoreceptors and nociceptors
A, the distribution of mechanically gated currents in the total population of neurones studied ($n = 158$) is shown in a pie chart. We have subdivided neurones with an RA current into type 1 and type 2 cells that are chiefly distinguished by the absence or presence of a hump on the falling phase of the action potential. Example traces of the measured action potential configuration for each cell type are shown together with the percentage of the total population adjacent to each pie chart slice. Scale bar for action potential correspond to 2 ms and 10 mV. *B*, the action potential width (measured at 50% amplitude) is plotted against the soma diameter for cells exhibiting RA, SA, IA or no mechanically gated current. Note that type 1 and type 2 cells with RA currents have very different cell sizes and action potentials widths ($P < 0.001$ unpaired *t* test for both parametres). RA type 2 and cells with IA currents had similar action potential widths but IA cells were significantly larger than RA type 2 cells ($P < 0.05$ unpaired *t* test). Cells with an SA current had significantly broader action potentials than RA type 1, RA type 2 and IA cells ($P < 0.001$ unpaired *t* test). *C*, the activation time constant τ_1 and the inactivation time constant τ_2 are plotted for RA type 1 and type 2 cells separately. It was clear that the RA type 1 cells have significantly faster activation and inactivation kinetics than type 2 cells (*$P < 0.02$ unpaired *t* test).

near 0 mV and displayed a linear slope conductance (see below).

Functional mechanosensitive conductances are concentrated on sensory neurites

Previous groups have carried out experiments using mechanical stimulation of the cell soma where a substantial proportion of cells do not possess a mechanically activated conductance (Cunningham *et al.* 1995; McCarter *et al.* 1999; Drew *et al.* 2002, 2004). We therefore decided to directly compare mechanically activated currents evoked from the soma with those evoked from the neurite. We sampled the same range of cell sizes as for the neurite stimulation experiments and applied a mechanical stimulus to the soma (Fig. 4 and Table 1). The probe was moved iteratively obliquely onto the cell soma. First single mechanical pokes identical to those used for the neurite (1.0 μm) were used. However, in all cases this small stimulus evoked no response. We therefore applied a series of larger stimuli by applying a 'staircase' of 1 μm steps in increasing number (2, 4, 6, 8, 16, etc.). This is a very similar mechanical stimulation protocol to that used by Drew *et al.* (2002, 2004), and in agreement with their results we mostly only obtained current responses with indentation stimuli > 4 μm on the cell body (median value, 6 μm; first quartile range, 6–8 μm). We also found that a substantial proportion of cells exhibited no current response to mechanical stimulation of the soma with any of the stimuli used (up to 32 μm) (Fig. 4). Thus only about 60% of the cells we tested with soma stimulation displayed a mechanically activated current (Fig. 4). In cases where no current was observed we repeatedly stimulated the soma using larger amplitude stimuli at different sites to be sure that no false-negatives were recorded. The proportion of cells with RA, SA and IA current responses was not different between the two sites of stimulation suggesting no one type of mechanosensitive current was lacking in the soma (Fig. 4). Indeed we found that the peak amplitude of the soma-evoked currents was also not significantly different from those evoked from the neurites for all three current types (Fig. 4 and Table 1). The effective stimulus amplitude required for somal currents was much larger than that at the neurite. Indeed in all cases studied, a visible membrane indentation of the soma could be observed concurrently with current activation. In each cell in which a somal current was evoked we also stimulated the neurite ($n = 55$). The type of current evoked from the soma

and neurite was always the same, thus if an RA current was evoked from the neurite then somal stimulation also evoked an RA current.

There was little difference in the mean amplitude of the current evoked from distant neurite sites, neurites immediately adjacent to the soma or the soma itself ($< 5\ \mu$m). This suggests there is only a slight attenuation of the current from the distant stimulation site (Table 1). As with mechanical stimulation of neurites adjacent to the soma, we found that the kinetic properties of somal currents were broadly similar to those found by stimulating the neurite. However, two kinetic parametres of the RA and SA current differed significantly in the soma from those found with neurite stimulation: the mean inactivation time of the RA soma current was 30% faster and the mean activation time constant of the SA soma current was faster than from the neurite (Table 1). In the former case it may be that this apparent difference between soma and neurite arises simply because a large proportion of RA type 1 cells were recorded (8/16 cells) which clearly have faster activation kinetics (Fig. 3*C*).

It might be argued that the absolute threshold for mechanically gated currents in the neurite is nevertheless equivalent to that found in the soma. For example, the change in curvature of the membrane required to activate the current might be equivalent and so the geometry of the stimulated object, a tube-like neurite or spherical cell body, might influence the apparent displacement threshold for the current. We cannot address this issue directly as changes in force or curvature cannot be directly measured during the stimulus. Nevertheless, in order to address the absolute sensitivity of the mechanosensitive channels in the neurite membrane we used the fine mode of the nanomotor where a single step corresponds to around 1 nm. The stimulating pipette tip was placed as close to the neurite as possible and a staircase of fine steps (250, 500, etc.) were applied from this starting position. For neurites with an RA current the first significant mechanically gated currents were observed with 250 steps (equivalent to 250 nm) and the current size increased with increasing stimulus strength (Fig. 4*E*). It is interesting that the maximal peak current amplitude was not significantly different from that observed with the coarse step (Fig. 4*F*). The mean size of the neurite at the point of stimulation for all stimulated neurites was $2.53 \pm 0.15\ \mu$m, as measured from pictures of all Lucifer Yellow-filled neurones. Thus we can conclude at least for the RA current that an indentation equivalent to a maximum of 10% of the neurite diameter is sufficient to activate mechanosensitive channels.

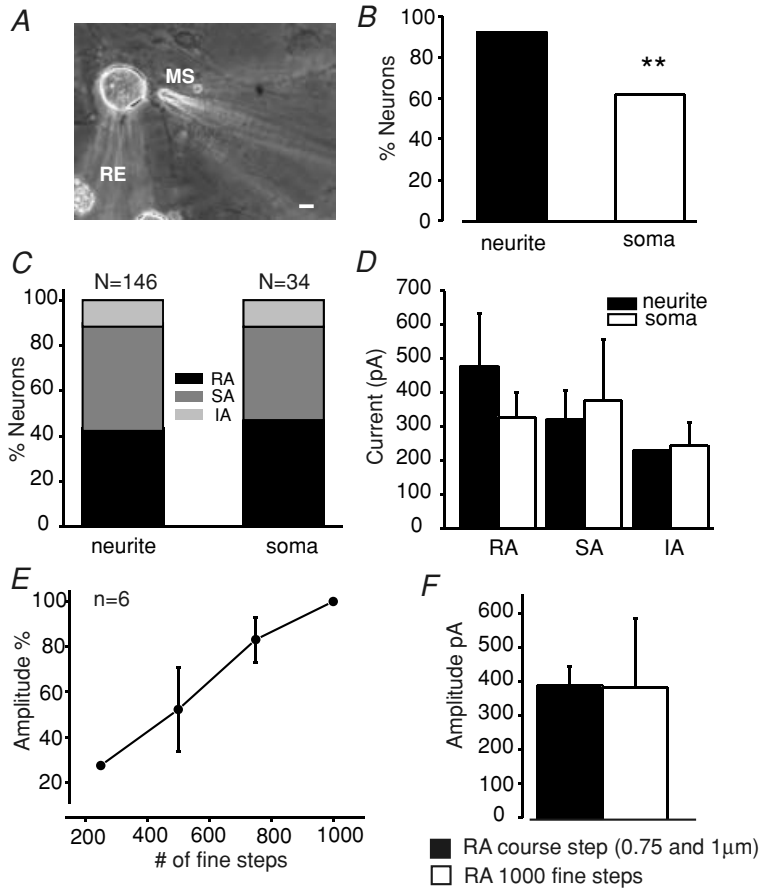

Figure 4. Comparison of mechanically evoked currents in the soma and neurite
A, the photomicrograph shows an example of the recording and stimulation procedure for evoking somal currents. Scale, 10 μm. *B*, the proportion of cells in which any mechanically evoked current could be evoked in the soma was significantly smaller ($P < 0.001$, χ^2 test) than that found in the neurite. *C*, when we analysed the proportion of only those cells with a mechanosensitive current, the incidence of the RA, SA and IA current was not different. *D*, the mean amplitude of the mechanically gated currents evoked from the soma was also not significantly different from that found in the neurite. The data plotted are only from cells that were tested with a mechanical stimulus at the neurite and at the soma ($n = 55$). The amplitude of the displacement stimulus needed to evoke a somal current was many times larger than that used for neurites (see text). *E*, in some cells we also used smaller displacement stimuli (range, ~250–1000 nm) applied to the neurite using the fine mode of the nanomotor. An analysis of six cells with an RA type current revealed that increasing displacement starting from 250 nm produced increasing current amplitudes in the same cells. *F*, for supratheshold stimuli the mean magnitude of the RA current was found to be the same regardless of whether the fine or coarse mode was used.

More than one type of mechanically gated channel in sensory neurones

The kinetics of mechanically gated currents in different sensory neurones can be quite different (Fig. 1*B*). This raises the question of whether mechanically activated currents with different kinetics reflects the activation of uniform populations of ion channels or not. One way to address this is to ask whether the reversal potential or pharmacological sensitivity of the currents differ. Thus we measured the reversal potential of the SA and RA current evoked by either stimulating the cell soma or the neurite very close to the cell soma. In this recording configuration we could assume that the membrane potential at the site of stimulation was under voltage clamp. The mechanical stimulus was then delivered with the membrane command voltage set manually to various membrane potentials between −60 and +100 mV. For each cell the mechanically activated current was activated at two to four holding potentials. A linear fit of the data taken from cells with an RA current ($n = 13$) indicated that the current reverses at very positive potentials (∼80 mV) (Fig. 5*A*). In contrast, equivalent data obtained from cells displaying an SA current ($n = 8$) indicated a non-selective cation current reversing at ∼+7 mV (Fig. 5*B*). The very positive extrapolated reversal potential of the RA current is highly reminiscent of mechanosensitive channels with a very high relative sodium permeability (Hoger *et al.* 1997). In order to test this idea more directly, mechanically gated currents were also tested in solutions where sodium ions were replaced by the non-permeant cation *N*-methyl D-glucamine (NMDG+) at a holding potential of −60 mV. Consistent with the idea that the RA current is sodium selective, practically no current was observed under these conditions (Fig. 5*C*). In contrast, replacing extracellular sodium by $NMDG^+$ failed to block SA currents measured at −60 mV (Fig. 5*C*). These experiments demonstrate that the ionic selectivity of RA and SA currents is indeed quite different. We also obtained reversal potential data from one cell with an IA current. Measurement of the current at four different holding potentials (−60 to +60 mV) indicated that the current–voltage (*I–V*) relation was linear with reversal at +33 mV.

We used drugs to probe the pharmacological sensitivity of the current that we recorded after stimulation of neurites. We found, like others (Drew *et al.* 2002), that gadolinium (10 μM) was effective at blocking the mechanically activated conductance (SA, $n = 2$ cells; RA, $n = 2$ cells; IA, $n = 1$ cell) with recovery of the current observed after washout (Fig. 7). Sensitivity to gadolinium is a feature of most other mechanically sensitive channels recorded in sensory cells so far (Erxleben, 1989; McCarter *et al.* 1999; Cho *et al.* 2002; Drew *et al.* 2002; Strassmaier & Gillespie, 2002). In order to probe the putative molecular identity of the channel we used drugs that have been reported to be selective for candidate mechanosensitive channels belonging to the Deg/ENaC family or the TRP families of channels (Drew & Wood, 2005; Lin & Corey, 2005; Hu *et al.* 2006). We used the potent amiloride analogue benzamil (100 μM) that can block Deg/ENaC

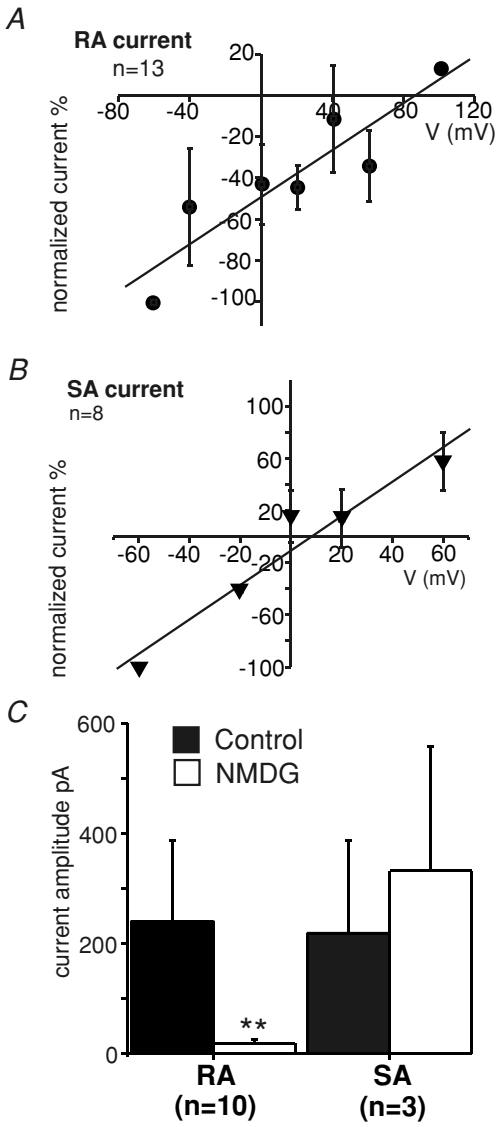

Figure 5. Heterogeneity of mechanically gated currents in sensory neurites
A, current–voltage relations for the mechanically activated current evoked by stimulating the cell soma or neurite immediately adjacent to the soma. In the case of cells with an RA current ($n = 13$), a linear fit of the data indicated that the current reverses at around +80 mV. Note both RA type 1 and type 2 cells were included in this analysis and no difference was seen in their *I–V* relation. *B*, in contrast, for data obtained from cells with an SA response ($n = 8$), a linear fit indicated reversal at or slightly positive to 0 mV. *C*, replacement of sodium ions in the extracellular solution by the non-permeant cation $NMDG^+$ completely blocked the RA current ($n = 10$) measured at −60 mV. No significant effect of $NMDG^+$ ions was observed on the SA current ($n = 3$).

channels and ruthenium red (10 μM) that has a broad spectrum of activity on most TRP channels tested so far. These drugs were superfused over the mechanically stimulated neurite or in a second series of experiments the drug was added to the extracellular solutions and mechanosensitive currents measured in the presence of the drug and compared to those found in control cultures. We found that ruthenium red had no significant effect on the amplitude of the RA current but could significantly reduce the amplitude of the SA current (Fig. 6*A* and *C*). Full recovery of the SA current amplitude was observed after drug washout (Fig. 6*C*). In contrast, benzamil (100 μM) had no effect on the amplitude of either the RA or SA current (Fig. 6*B* and *D*). However, we noticed that after exposure to benzamil the latency for current activation in cells with both an RA and SA current increased by up to 3-fold (Fig. 6*B* and *D*), this effect was reversed after removal of benzamil; no such effects on mechanical latency were observed with ruthenium red (Fig. 6*B* and *D*). We also measured cells that had been chronically exposed to benzamil (100 μM) for between 30 and 180 min. Here we also observed no effect on the mean amplitude of either the RA or SA current (Fig. 6*E*). The latency for current activation was, however, markedly increased for cells with an RA or SA current, in the case of cells with an RA current the latencies increased by an average of 7-fold in the presence of benzamil (Fig. 6*F*).

The neurites of a single cell were often mechanically stimulated at different locations and in the vast majority of cases the same type of current was observed at each location (91%, 128/140 cells). However, we did find in rare cases (9%, 12/140 cells) that both RA and SA type responses could be evoked separately from different stimulation sites on the same neurone. The cells that we found with two types of currents at different locations were all nociceptors as defined by the criteria outlined above (Fig. 7). It should

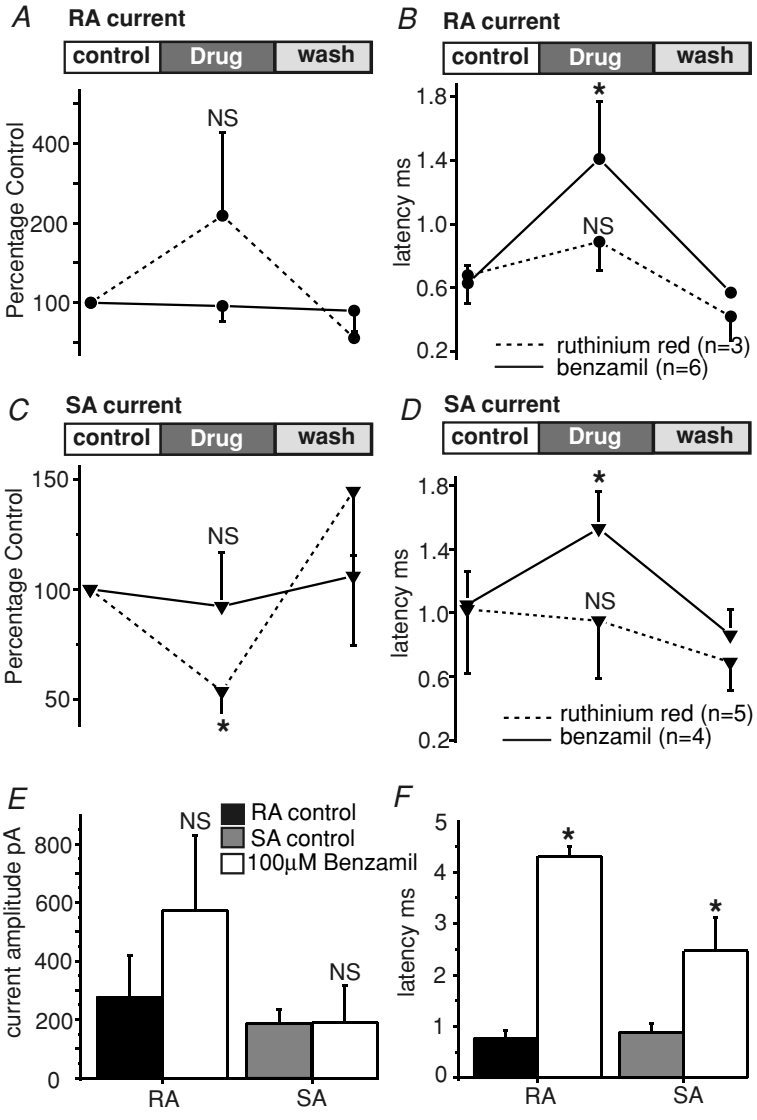

Figure 6. Differential pharmacological sensitivity of SA and RA currents in sensory neurites
A, cells with an RA current were incubated with 10 μM ruthenium red ($n = 3$) or 100 μM benzamil ($n = 6$) and the current amplitude measured before, during and after drug application. No significant effect of ruthenium red on the current amplitude was noted. *B*, the kinetic parameters of the RA current was also monitored during drug application and a significant increase in the latency for current activation was found in the presence of benzamil but not ruthenium red. *C*, in contrast to the RA current the mean amplitude of the SA current could be partially blocked by 10 μM ruthenium red ($n = 5$); 100 μM benzamil again had no significant effect on the current ($n = 4$). *D*, benzamil but not ruthenium red caused a significant and reversible increase in the latency for SA current activation. *E*, mechanically gated currents were measured in the continued presence of 100 μM benazamil. The amplitude of SA ($n = 9$) and RA ($n = 9$) currents were not significantly affected by the presence of benzamil. *F*, the latency for current activation was dramatically changed in the presence of benzamil with latency increasing more than 5-fold in the case of RA cells (*$P < 0{,}05$ unpaired t test).

be pointed out that because the speed of activation τ_1 of the RA and SA current is identical (Table 1), it is quite possible that nociceptors occasionally possess a small RA current that is masked by the SA current.

Discussion

At the heart of our mechanosensory experience is the mechanism whereby somatic sensory neurones rapidly transduce mechanical stimuli. The identity(ies) of the sensory transduction channels and the molecular requirements for their mechanosensitivity are not known. In this study we have established a new *in vitro* model where mechanically gated currents with activation thresholds and physiological properties reminiscent of the *in vivo* situation can be studied. We provide good evidence that displacement stimuli in the submicrometre range can directly open ion channels present in sensory neurone neurites. The mechanosensitive conductances that we observe can be easily classified according to their kinetic properties into one of three types termed in the present study RA, SA and IA. Furthermore, based on clear differences in the reversal potential and pharmacological sensitivity of RA and SA currents, it seems likely that there are at least two molecular entities of mechanically gated channel that underlie the observed currents.

It is important at the outset to make sure that the observed mechanosensitive currents are not artefacts (e.g. a leak conductance initiated by the mechanical stimulus). We believe this is very unlikely to be the case for any of the three types of currents described. Firstly, the currents could be evoked repetitively from the neurite with little evidence of attenuation with repeated trials. Secondly, the currents measured had distinctive I–V relations, which in the case of the RA current cannot be explained by simple membrane leak. Finally, we have shown that at least one pharmacological agent can reversible block or modulate all three types of current.

Physiological significance of mechanically gated currents in sensory neurones

Many cutaneous mechanoreceptors are capable of detecting skin displacements in the order of tens of micrometres as illustrated by psychophysical measurements in man and other primates (Johnson, 2001; Romo & Salinas, 2003). A striking example of the speed of somatosensation is how phase-locked cortical activity can be observed within 50 ms of the onset of somatic stimulation despite the cortex being physically distant and at least three synaptic relays away from the site of transduction (Romo & Salinas, 2003). The speed and sensitivity of mechanotransduction is all the more surprising as it is known that the mechanosensitive endings of most sensory neurones are embedded in tissue some hundreds of micrometres from the surface of the skin. This fact illustrates an enduring problem of studying somatic sensory mechanotranduction; that is, the near impossibility of quantitatively stimulating the sensory membrane directly *in vivo*. Mechanotransduction by hair cells of the inner ear can in contrast be studied very directly by moving the stereocillia tips in *ex vivo*

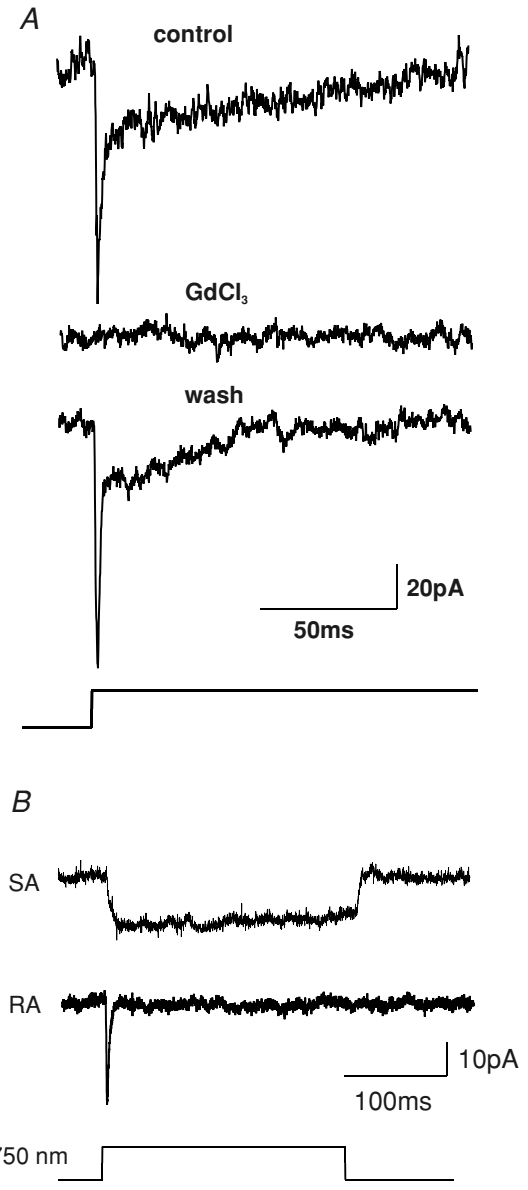

Figure 7. Sample traces illustrating reversible blockade of the mechanosensitive current by gadolinium and presence of RA and SA currents in single cells

A, sample traces before, during and after incubation of the cell with gadolinium (10 μM). Note that the current is completely and reversible blocked by gadolimium. *B*, example traces recorded by stimulating the neuritic tree of a single sensory neurone at two locations. In rare cases, such as illustrated, an SA or RA current were evoked at the two locations.

preparations (Markin & Hudspeth, 1995; Strassmaier & Gillespie, 2002). Here we have established a new *in vitro* model of sensory mechanotransduction that features a very high level of sensitivity and speed expected of the *in vivo* sensory ending. The mechanical displacement of the neurites of freshly cultivated sensory neurones reliably evokes a mechanically activated current, which can be measured with little apparent attenuation at the soma (Table 1). In our experiments, we cannot determine the absolute displacement threshold for this current as the standard step stimuli were initiated an unknown distance from the neurite membrane. Thus when a step size of 750 nm was used, as in most experiments, the probe might theoretically impact the neurite at any point during its travel. We can assume that the start position of the probe is a random variable and it follows that the average plasma membrane displacement might be around 370 nm assuming the current activates very soon after contact with the membrane. Our observation that virtually every neurite tested displays mechanically gated currents with a large mean amplitude suggests that this stimulus was suprathreshold. We also addressed this point directly by showing that the RA current amplitude codes the amplitude of the displacement in a range from 250 to 1000 nm (Fig. 4*E*). The extraordinary sensitivity of the neurite mechanically activated current is in sharp contrast to very similar currents found after stimulation of the cell body of sensory neurones in culture (McCarter *et al.* 1999; Drew *et al.* 2002, 2004). Mechanically activated currents evoked by prodding the cell soma have displacement thresholds an order of magnitude higher than those reported here for the neurite (Fig. 4). The mean size of the neurite that we have stimulated in our experiments was 2.5 μm. In principle, it is therefore possible that the deformations of the tube-like neurite by the stimuli are similar to those produced on the soma in terms of the percentage change in membrane curvature. We cannot at present with our methods directly test this idea, as we cannot directly measure force or membrane curvature during the stimulus. Nevertheless the fact that 40% of cells stimulated at the soma never show mechanically gated currents strongly suggests that the effective stimulus is indeed smaller at the neurite membrane.

The kinetics of mechanically activated currents in the soma described by Drew *et al.* (2004) are very similar to those found here. They did not measure the latency or activation time constant of the different types of mechanically activated currents that they observed but the first inactivation time constant that they estimated for the RA-like current is in the range of the values that we find here (Table 1). Although the mechanical stimulation used by Drew and colleagues was similar to that used here, one important difference is that the speed of probe movement used here was up to 20 times faster (10 μm ms^{-1} compared to 0.5 μm ms^{-1}). The small differences in the kinetic properties of the current might therefore be due to an inherent dependence of the underlying channels on the speed of stimulation.

A fundamental question remains of whether the properties of the recorded mechanosensitive currents in culture reflect qualitatively and quantitatively the properties of the transduction apparatus *in vivo*. This question is difficult to answer, as it has proved impossible to measure the transduction current in intact mammalian sensory neurones *in vivo* (Hu *et al.* 2006). It must also be kept in mind that cultured sensory neurones have recently been axotomised, and that axotomy and the ensuing regeneration response clearly affect the mechanosensitivity of sensory neurones. Very soon after primary afferents reinnervate the skin, receptive properties are often immature and single afferent fibres are either unresponsive or are only activated by brisk tap stimuli (Terzis & Dykes, 1980; Pover & Lisney, 1988). In addition, the mechanosensitive properties of afferent endings trapped in a nerve neuroma are also immature and indeed never match the mechanosensitivity of afferents that have successfully reinnervated the skin (Michaelis *et al.* 1995, 1999).

Heterogeneity of mechanoreceptors and mechanosensitive currents

The DRG contains a large variety of sensory neurones with a mechanoreceptive function (Lewin & Moshourab, 2004). It is not clear whether all these different mechanoreceptors utilize the same mechanosensitive channels and transduction components. Based on the kinetics of inactivation of the mechanically activated currents, we could classify them into one of three types: RA, IA and SA (Fig. 1). It was clear that mechanoreceptors with large cell bodies and narrow action potentials express an RA current but this current is also observed in a population of small cells with broader action potentials (Fig. 3). For this reason we have subdivided cells with an RA current into type 1 and type 2 cells. It was interesting that kinetics of activation and inactivation seen for the RA current in type 1 (mechanoreceptor) are significantly faster than those observed in type 2 (nociceptive) cells. This may mean that the underlying channels in these cells differ in their subunit composition. We have, however, found no clear biophysical difference between the RA current in type 1 and type 2 cells. The intermediate nature of the RA type 2 cell properties is reminiscent of the recently described Aβ-nociceptors (Woodbury & Koerber, 2003; Djouhri & Lawson, 2004; Fang *et al.* 2005).

Previous authors suggested that the mechanosensitive conductance observed in the cell soma is non-selective for cations (McCarter *et al.* 1999; Drew *et al.* 2004). However, here we find that the *I–V* relation of mechanically activated

conductance with different inactivation kinetics is indeed quite distinctive for the SA and RA current (Fig. 5). Thus the RA current showed a linear I–V relation with reversal in physiological salt solutions at ∼+80 mV (Fig. 5). The current was also completely abolished when extracellular Na^+ ions were replaced by the impermeant cation $NMDG^+$ (Fig. 5). The SA current showed clear reversal around 0 mV under identical conditions indicating that a non-selective channel may underlie this current. The SA but not the RA current was also partially blocked by the TRP channel antagonist ruthenium red (Fig. 6). No sign of strong outward rectification was observed for the SA current; a feature often noted with TRP channels, such as TRPV1, TRPV2 and TRPA1 which are expressed by nociceptors (Clapham *et al.* 2005). We also tested the sensitivity of mechanosensitive currents to benzamil, which is a potent amiloride-like compound that can block members of the Deg/ENaC channel family (Drew *et al.* 2004). We also noted no significant block of any mechanosensitive current in the presence of benzamil; however, this compound reversibly increased the latency for current gating (Fig. 6). At the present time, we do not have a mechanistic explanation for this interesting effect.

Conclusions

In this study we show for the first time that acutely cultivated sensory neurones possess mechanosensitive currents in their neurites with sensitivities to displacement stimuli in the submicrometre range. The distinctive biophysical properties of RA and SA currents that are predominantly found in mechanoreceptive and nociceptive neurones are highly suggestive of distinct underlying ion channel entities. Our data suggest that the neurite of acutely cultured sensory neurones can serve as a convenient experimental model of the mechanosensitive sensory ending *in vivo*.

References

Akopian AN, Sivilotti L & Wood JN (1996). A tetrodotoxin-resistant voltage-gated sodium channel expressed by sensory neurons. *Nature* **379**, 257–262.

Cho H, Koo JY, Kim S, Park SP, Yang Y & Oh U (2006). A novel mechanosensitive channel identified in sensory neurons. *Eur J Neurosci* **23**, 2543–2550.

Cho H, Shin J, Shin CY, Lee SY & Oh U (2002). Mechanosensitive ion channels in cultured sensory neurons of neonatal rats. *J Neurosci* **22**, 1238–1247.

Clapham DE, Julius D, Montell C & Schultz G (2005). International Union of Pharmacology. XLIX. Nomenclature and structure-function relationships of transient receptor potential channels. *Pharmacol Rev* **57**, 427–450.

Cunningham JT, Wachtel RE & Abboud FM (1995). Mechanosensitive currents in putative aortic baroreceptor neurons in vitro. *J Neurophysiol* **73**, 2094–2098.

Di Castro A, Drew LJ, Wood JN & Cesare P (2006). Modulation of sensory neuron mechanotransduction by PKC- and nerve growth factor-dependent pathways. *Proc Natl Acad Sci U S A* **103**, 4699–4704.

Djouhri L & Lawson SN (2004). Abeta-fiber nociceptive primary afferent neurons: a review of incidence and properties in relation to other afferent A-fiber neurons in mammals. *Brain Res Brain Res Rev* **46**, 131–145.

Drew LJ, Rohrer DK, Price MP, Blaver KE, Cockayne DA, Cesare P & Wood JN (2004). Acid-sensing ion channels ASIC2 and ASIC3 do not contribute to mechanically activated currents in mammalian sensory neurones. *J Physiol* **556**, 691–710.

Drew LJ & Wood JN (2005). Worm sensation! *Mol Pain* **1**, 8.

Drew LJ, Wood JN & Cesare P (2002). Distinct mechanosensitive properties of capsaicin-sensitive and -insensitive sensory neurons. *J Neurosci* **22**, RC228.

Erxleben C (1989). Stretch-activated current through single ion channels in the abdominal stretch receptor organ of the crayfish. *J Gen Physiol* **94**, 1071–1083.

Fang X, McMullan S, Lawson SN & Djouhri L (2005). Electrophysiological differences between nociceptive and non-nociceptive dorsal root ganglion neurones in the rat in vivo. *J Physiol* **565**, 927–943.

Gillespie PG & Walker RG (2001). Molecular basis of mechanosensory transduction. *Nature* **413**, 194–202.

Hoger U, Torkkeli PH, Seyfarth EA & French AS (1997). Ionic selectivity of mechanically activated channels in spider mechanoreceptor neurons. *J Neurophysiol* **78**, 2079–2085.

Hu J, Milenkovic N & Lewin GR (2006). The high threshold mechanotransducer: a status report. *Pain* **120**, 3–7.

Hunt CC & Ottoson D (1973). Receptor potential and impulse activity in isolated mammalian spindles. *J Physiol* **230**, 49–50*P*.

Johnson KO (2001). The roles and functions of cutaneous mechanoreceptors. *Curr Opin Neurobiol* **11**, 455–461.

Koerber HR, Druzinsky RE & Mendell LM (1988). Properties of somata of spinal dorsal root ganglion cells differ according to peripheral receptor innervated. *J Neurophysiol* **60**, 1584–1596.

Lawson SN, Crepps BA & Perl ER (1997). Relationship of substance P to afferent characteristics of dorsal root ganglion neurones in guinea-pig. *J Physiol* **505**, 177–191.

Lewin GR & Moshourab R (2004). Mechanosensation and pain. *J Neurobiol* **61**, 30–44.

Lin SY & Corey DP (2005). TRP channels in mechanosensation. *Curr Opin Neurobiol* **15**, 350–357.

Lindsay RM (1988). Nerve growth factors (NGF, BDNF) enhance axonal regeneration but are not required for survival of adult sensory neurons. *J Neurosci* **8**, 2394–2405.

Loewenstein WR & Skalak R (1966). Mechanical transmission in a Pacinian corpuscle. An analysis and a theory. *J Physiol* **182**, 346–378.

McCarter GC, Reichling DB & Levine JD (1999). Mechanical transduction by rat dorsal root ganglion neurons in vitro. *Neurosci Lett* **273**, 179–182.

Mannsfeldt AG, Carroll P, Stucky CL & Lewin GR (1999). Stomatin, a MEC-2 like protein, is expressed by mammalian sensory neurons. *Mol Cell Neurosci* **13**, 391–404.

Markin VS & Hudspeth AJ (1995). Gating-spring models of mechanoelectrical transduction by hair cells of the internal ear. *Annu Rev Biophys Biomol Struct* **24**, 59–83.

Michaelis M, Blenk KH, Janig W & Vogel C (1995). Development of spontaneous activity and mechanosensitivity in axotomized afferent nerve fibers during the first hours after nerve transection in rats. *J Neurophysiol* **74**, 1020–1027.

Michaelis M, Blenk KH, Vogel C & Janig W (1999). Distribution of sensory properties among axotomized cutaneous C-fibres in adult rats. *Neuroscience* **94**, 7–10.

Pover CM & Lisney SJ (1988). An electrophysiological and histological study of myelinated axon regeneration after peripheral nerve injury and repair in the cat. *J Neurol Sci* **85**, 281–291.

Romo R & Salinas E (2003). Flutter discrimination: neural codes, perception, memory and decision making. *Nat Rev Neurosci* **4**, 203–218.

Shin JB, Martinez-Salgado C, Heppenstall PA & Lewin GR (2003). A T-type calcium channel required for normal function of a mammalian mechanoreceptor. *Nat Neurosci* **6**, 724–730.

Strassmaier M & Gillespie PG (2002). The hair cell's transduction channel. *Curr Opin Neurobiol* **12**, 380–386.

Stucky CL & Lewin GR (1999). Isolectin B(4)-positive and -negative nociceptors are functionally distinct. *J Neurosci* **19**, 6497–6505.

Stucky CL, Rossi J, Airaksinen MS & Lewin GR (2002). GFR alpha2/neurturin signalling regulates noxious heat transduction in isolectin B4-binding mouse sensory neurons. *J Physiol* **545**, 43–50.

Terzis JK & Dykes RW (1980). Reinnervation of glabrous skin in baboons: properties of cutaneous mechanoreceptors subsequent to nerve transection. *J Neurophysiol* **44**, 1214–1225.

Wood JN, Boorman JP, Okuse K & Baker MD (2004). Voltage-gated sodium channels and pain pathways. *J Neurobiol* **61**, 55–71.

Woodbury CJ & Koerber HR (2003). Widespread projections from myelinated nociceptors throughout the substantia gelatinosa provide novel insights into neonatal hypersensitivity. *J Neurosci* **23**, 601–610.

Acknowledgements

This work was supported in part by grant SPP 1025 from the Deutsche Forschungsgemeinschaft to G.R.L. and a fellowship to J.H. from the Alexander von Humboldt Foundation. The excellent technical assistance of Anja Wegner and Heike Thränhardt is gratefully acknowledged. We would like to thank Thomas Park and Paul Heppenstall for constructive comments on an earlier manuscript.